metals

MDPI

Article

Dehydrogenation of AlSi7Fe1 Melt during In Situ Composite Production by Oxygen Blowing

Arkady Finkelstein [1,*], Arseny Schaefer [1] and Nikolay Dubinin [1,2]

[1] Department of Foundry Engineering and Strengthening Technologies, Ural Federal University, 620002 Ekaterinburg, Russia; a.a.shefer91@gmail.com (A.S.); ned67@mail.ru (N.D.)
[2] Institute of Metallurgy of the Ural Branch of the Russian Academy of Sciences, 620016 Ekaterinburg, Russia
* Correspondence: avinkel@mail.ru; Tel.: +7-912-205-5520

Abstract: The technology of producing a composite material in situ envisages the pre-saturation of an AlSi7Fe1 melt with hydrogen; afterwards, the melt is blown with oxygen until the hydrogen dissolved in the melt is burned out. The hydrogen content was researched during the manufacturing process of the composite material; before oxygen blowing, and at incomplete and complete burning out of the dissolved hydrogen. The interrelation between the absorbed hydrogen content and the aluminum oxide fraction was identified. A mathematical model was proposed which demonstrated that during the saturation process of the melt with oxide particles, hydrogen was absorbed on their surface as a layer close to monoatomic, which does not lead to the realization of the pores' heterogeneous nucleation mechanism. Due to this, castings produced from the researched composite material are leakless. Incomplete burning out of hydrogen dissolved in the melt leads to the formation of significant hydrogen porosity. The proposed method of prevention of gas porosity in cast composites is an alternative to the conventional one and offers not only the purging of the melt from oxide inclusions but, on the contrary, a significant increase in their specific surface, which allows for the reduction in hydrogen content on the inclusion surface to the monoatomic level.

Keywords: aluminum matrix composite (AMC); hydrogen; aluminum oxide; oxygen blowing; leakless casting

Citation: Finkelstein, A.; Schaefer, A.; Dubinin, N. Dehydrogenation of AlSi7Fe1 Melt during In Situ Composite Production by Oxygen Blowing. *Metals* **2021**, *11*, 551. https://doi.org/10.3390/met11040551

Academic Editors: Jacques Huot and Shusen Wu

Received: 13 February 2021
Accepted: 24 March 2021
Published: 28 March 2021

1. Introduction

At present, aluminum matrix composites are not only developed, but also commercially produced [1]. As is shown in paper [2], hydrogen porosity is the main problem in the production of aluminum matrix molded composites. In paper [3], the porosity of composites is divided into two types, that is, the phase boundary porosity and the matrix alloy porosity. The first type of porosity is especially dangerous, as it results in a loss of the bond between the strengthening particles and matrix metal, and deformation begins at small loads [4]. Sometimes, an insignificant porosity combined with strengthening by nanoparticles leads to unexpected effects, in particular, to a very large percentage elongation, which is, in general, uncharacteristic for composites [5] and is a consequence of Young's modulus decrease. The second type of porosity in a metal matrix originates from a significant decrease in hydrogen solubility in aluminum during crystallization [6].

The review of works [7] on the subject of pore formation in an aluminum alloy presents a picture of direct dependence of the pore volume on hydrogen percentage, whereas in the case of the equilibrium concentration at the crystallization temperature, the pore volume is equal to 3%. The paper also shows a direct dependence of the oxide particles' surface area on the formation of hydrogen porosity. The oxide particle surface is a solid support whereon hydrogen atoms settle out, and the generation of pores begins at their critical concentration, while deep over-saturation without the formation of pores can be possible at high purity (that is, low percentage of non-metallic inclusions) of the melt. Thus, according to numerous literature reports, inclusions provoke pore formation. Regarding composites,

it was comprehensively researched in paper [8], where the increase in porosity is shown at the increase in the strengthening component specific surface. On the other hand, paper [9] demonstrated the over-saturation of the aluminum alloy with hydrogen in the presence of oxide spots with a large area.

Techniques which are conventionally used for purging aluminum melts from hydrogen —that is, inert or active gas flushing–cannot be utilized in the aluminum composite technology due to the strengthening component sedimentation. So, the degassing of raw-stock materials becomes the main way to solve the gaseous porosity issue.

The technology of producing the oxide aluminum composite in situ developed by the authors envisages the oxygen blowing of the pre-hydrogenated AlSi7Fe1 melt [10]. The gist of the process is presented in Figure 1.

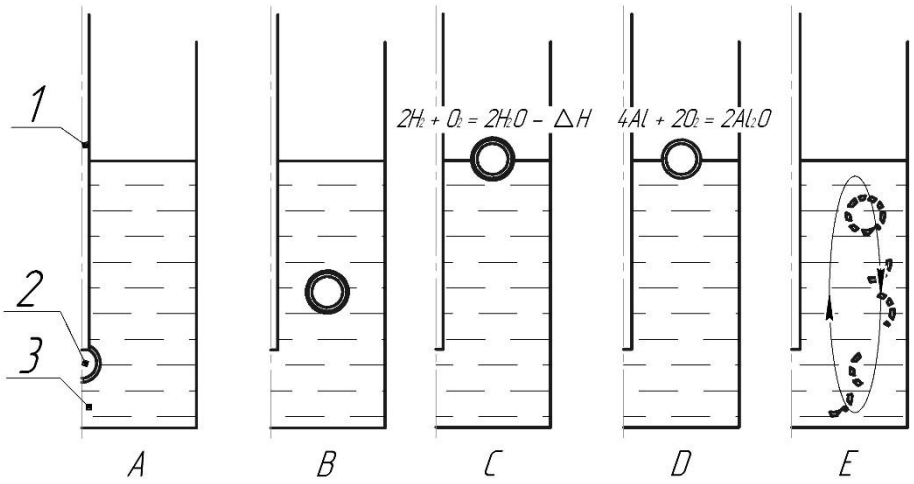

Figure 1. The process diagram: 1. Tuyere. 2. Oxygen bubble. 3. Aluminum alloy melt. (**A**)—bubble formation; (**B**)—bubble flotation, hydrogen is adsorbed on it; (**C**)—hydrogen burning on the melt mirror; (**D**)—formation of aluminum gaseous suboxides; (**E**)—bubble disintegration, oxide particles saturate the melt

Before blowing, the melt is saturated with hydrogen by introducing titanium hydride (TiH_2). In the process of blowing, an oxygen bubble is formed on the tuyere flat; from inside, the mentioned bubble is covered with an aluminum oxide film (Figure 1A). As the oxygen bubble floats up, dissolved hydrogen is adsorbed on it (Figure 1B). The oxide film is impenetrable for hydrogen, so an interaction between hydrogen and oxygen in the bubble does not occur. The adsorbed hydrogen reacts with the furnace atmosphere oxygen on the melt mirror, giving release to energy (Figure 1C). The melt hydrostatic pressure drops at the floating, which results in the oxygen bubble expansion and formation of cracks therein. Hydrogen burning leads to the local heating of the melt up to temperatures above 980 ± 5 °C; at this temperature and oxygen deficiency, the reaction of formation of aluminum gaseous suboxides proceeds [11] in the oxygen bubble cracks (Figure 1D). As a result, the bubble gets disintegrated on the melt mirror, and the oxide film residues reinforce the melt (Figure 1E). To produce the consistent composite, disintegration of the oxide should only occur on the melt surface [12].

Methods of oxide bubble destruction within the volume of the melt are known. It is impossible to "heal" cracks in the oxide film due to the reduction in the oxygen percentage in the gas mixture [13] and the heating of the melt up to temperatures above 980 °C, which, as it was mentioned earlier, leads to the formation of aluminum gaseous suboxides [14]. However, the collapse of bubbles within the volume of the melt does not result in an improvement in strength of a produced alloy because of oxide porosity [15]. For the elimination thereof, it is necessary to destruct oxide bubbles, not within the volume of the melt, but on its mirror [12], thus, ensuring residual oxygen emission into the furnace

atmosphere. This is the very thing which allows the realization of preliminary saturation of the melt with hydrogen.

The obtained composite material shows much higher mechanical properties than the initial alloy. The ultimate tensile strength rises from 127 to 175 MPa in the as-cast condition; it is also characterized by the brittle failure pattern, that is, the practically complete absence of relative elongation [16].

The composite structure which determines its mechanical and functional properties is examined in detail in paper [17]. Oxide inclusions—mostly of the isotropic form—with size up to 100 nm are modifiers of the structure and provide refinement of eutectic phases and subgrains of the alpha-solid solution. The composite contains some small quantity of larger inclusions in the form of films and bi-films. The composite also showed complete absence of hydrogen porosity, despite the preliminary saturation of the alloy with hydrogen. This effect was applied when producing the cast item "pneumatic bulb" (Figure 2) at LLC Uraltsvetlit by die-casting, ensuring the complete absence of defects in terms of hydro permeability, whereas fabrication of the casting from conventional commercial alloy AlSi7 (A356) resulted in 30–40% of the products being faulty.

Figure 2. Cast item "Pneumatic bulb" from composite.

In the process of blowing, hydrogen is spent by burning on the melt mirror, thus, providing for local overheating and the destruction of oxygen bubbles on the surface necessary for the formation of the composite material. In the absence of hydrogen, oxygen blowing of the melt, as it is offered in [18], results in the formation of large-size oxide films and, consequently, the inability to use the produced material as structural. Upon the complete burning out of hydrogen dissolved in the melt, oxide bubbles floating up on the surface cease to be destroyed, and slag builds up on the melt mirror, which is a visual signal to discontinue the process of blowing. This study aims to determine the residual content of hydrogen in the melt.

2. Materials and Methods

To prepare specimens, a shaft-type resistance furnace (UrFU, Ekaterinburg, Russia) was used wherein a 0.5 L marshalite crucible (JSC Dinur, Pervouralsk, Russia) was installed and a blowing tuyere (JSC Dinur, Pervouralsk, Russia) from fused quartz with ID (Inner diameter) 6 mm and OD (Outside diameter) 10 mm was secured. Commercial-grade silumin AlSi7Fe1 (LLC Uraltsvetlit, Kamensk-Uralsky, Russia) (AK7 according to standard [19]) was used as a furnace charge, with a weight of 500 g $\pm$ 1 g. Hereinafter in this paper, measurements of solid substance masses were performed on scales AND GF-4000 and AND GR-300 (Ltd. A&D Company, Toshima, Japan). The alloy chemical composition is shown in Table 1 (measurement error $\pm$0.05%).

Table 1. Chemical composition of the experimental alloy.

Element	Al	Si	Mn	Fe	Mg	Cu	Zn	Ti
Casting alloy	Balance	6.79	0.38	1.08	0.54	0.73	0.45	0.15

The alloy was overheated to 1023 $\pm$ 1 K (750 $\pm$ 1 °C). For the hydrogenation of the melt, titanium hydride (II) (LLC UralInvest, Izhevsk, Russia) was used, which is usually applied for this purpose [20].

The equilibrium limit of hydrogen solubility was determined for the alloy with the chemical composition shown in Table 1 and for the abovementioned temperature on the basis of the data [21], where the system of hydrogen equilibrium solubility correction coefficients is dependent on the content of alloying and impurity elements is presented. The calculated hydrogen equilibrium content in the aluminum alloy melt is equal to 0.9124 ppm; thus, the required mass of titanium hydride is 0.01 g per 500 g of melt. The mass of titanium hydride introduced into the melt before blowing was taken with a significant exceedance of the solubility limit for the realization of local overheating in the process of blowing, as is mentioned above, that is, 1 $\pm$ 0.05 g. Consequently, the initial hydrogen content in the melt is 91 ppm.

To prevent the release of hydrogen during the introduction thereof, it was introduced into the melt wrapped in aluminum foil by means of an alloying basket. Still, a portion of hydrogen burns out as soon as is introduced into the melt in titanium hydride. Then the melt was blown with oxygen (JSC Linde UralTechGas, Ekaterinburg, Russia) with a constant flowrate about 0.063 m^3/h (measurement error $\pm$2.5%) determined by means of a mass flowmeter (industrial rotameter). The time of the complete burnout of hydrogen was not definitely established, but was identified by an acute growth of slag on the metal mirror, which was monitored visually. As our experience shows, the time of blowing with the mentioned flowrate until completion of hydrogen burning out is about 1 h, so the following heats were performed:

1. Without blowing, with the introduction of titanium hydride only.
2. With 30 min of blowing (incomplete hydrogen burn out).
3. With blowing until complete hydrogen burn out (5 heats).

Upon completion of blowing, the melt was poured into a green sand mold. From the produced castings (Figure 3), specimens were cut for studying. Three specimens were taken from each heat.

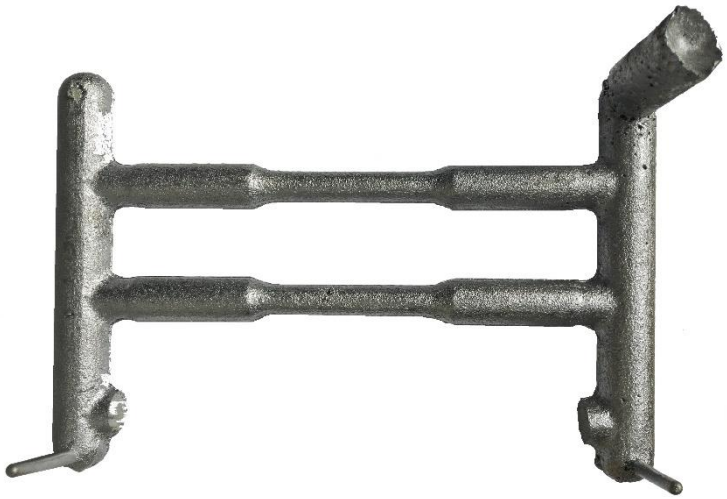

Figure 3. Casting of the aluminum matrix composite.

The fraction of aluminum oxide in specimens was determined by a technique [22] which involved dissolving the aluminum alloy in a mixture of potassium bromide, potassium and ethyl acetate. The hydrogen concentration in the specimens was studied on ELTRA ONH-2000 m. Most frequently, hydrogen content in metal is estimated in the literature in mL/100 g. ELTRA ONH-2000 m outputs readings of hydrogen concentration in mass fractions ppm. The conversion is performed on hydrogen mass in 1 cm^3, that is, 0.000089 g. Thus, 1 cm^3/100 g = 0.00000089 = 0.89 ppm.

Metallographic studies of specimens with the purpose of finding porosity were made with the use of an Olympus BX-51 optical microscope.

3. Results and Discussion

The hydrogen content found in the specimens and the aluminum oxide fraction are shown in Table 2.

Table 2. Hydrogen content and aluminum oxide fraction.

Heat	Hydrogen Content, ppm	Aluminum Oxide fraction, %
Without blowing	10.85 ± 0.5	>0.10
Incomplete blowing	12.60 ±0.5	1.9 ± 0.05
Full blowing 1	26.30 ± 0.5	5.1 ± 0.1
Full blowing 2	22.60 ± 0.5	4.3 ± 0.1
Full blowing 3	24.00 ± 0.5	4.8 ± 0.1
Full blowing 4	22.60 ± 0.5	4.6 ± 0.1
Full blowing 5	24.10 ± 0.5	4.8 ± 0.1

A polished section of the specimen blown until hydrogen fully burns out (Figure 4A) is not free from porosity. The pore size is up to 200 μm. The pore surface is oxide-coated, the thickness thereof is significant and characteristic for formation in the melt [17]. Contrary to hydrogen pores, the thickness of oxide on the surface whereof is significantly lower, that is, the pores are formed due to the incomplete collapse of an oxygen bubble in process of blowing. The non-round form of the pores is one more sign of their oxygen-based origin. The dendrite porosity area adjoins the pore around the alpha-solid solution; the mentioned pore possesses an obvious shrinkage origin and occurs in the crystallization interval, as a result of non-permeability of the oxide film for the melt. The oxide porosity is of a local nature and, naturally, reduces the composite mechanical properties to some extent, but does not influence hydro permeability.

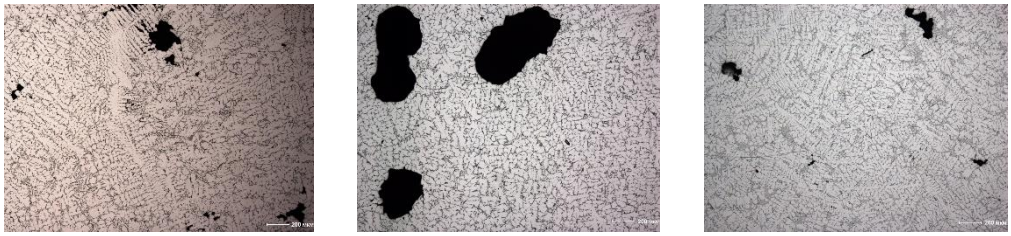

(**A**) (**B**) (**C**)

Figure 4. Casting of aluminum matrix composite. (**A**) Composite, blowing to the full burn out of hydrogen; (**B**) Composite, incomplete burn out of hydrogen; (**C**) Alloy without blowing.

Hydrogen in the composite, upon completion of the burning on the melt mirror can only be in the bound state, adsorbed on the aluminum oxide surface. The dependence of the hydrogen content in the composite may be presented graphically (Figure 5), the linear trend is described by Equation (1):

$$\%\ H_2\ (\text{content ppm}) = f\ (\%\ Al_2O_3) = 4.\ 7069 \times (\%\ Al_2O_3) + 1.7034 \quad (1)$$

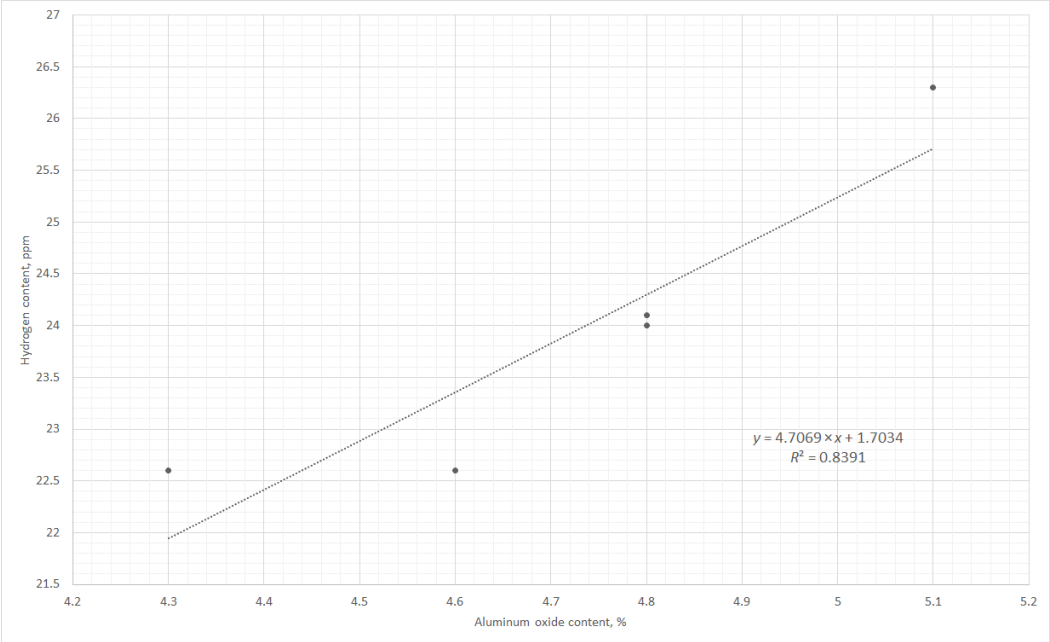

Figure 5. Dependence of the hydrogen content in a composite on aluminum oxide fracture.

The remaining term characterizes over-saturation of the melt with hydrogen under conditions of the absence of solid particles, that is, conditions for the pores' heterogeneous nucleation. In paper [23], over-saturation of an Al-Cu system alloy with hydrogen to 0.43 mL/100 g is shown, which corresponds to 0.48 ppm, i.e., significantly higher than the known equilibrium level associated with heterogeneous nucleation. However, the level of the melt's possible oversaturation in the absence of heterogeneous nucleation is not the main topic of the presented study, and a much larger quantity of experiments will be required for the clarification of this parameter.

In the examined literature, the interrelation between hydrogen content and aluminum oxide content [24] is presented quite often, similar to that presented in Figure 4. However, such an approach is feasible only for certain geometrical dimensions of oxide particles, as hydrogen absorption occurs on its active surface. At the same time, as it is well known, thickness of oxide films on aluminum may vary from nanometers to micrometers, depend-

ing on the conditions of their formation [25]. Influence of the shape and size of oxide spots on hydrogen content in the melt and formation of gaseous porosity is researched in paper [26].

As we see from results of paper [17], aluminum oxide particles in the composite under consideration have the shape which is close to isotropic. At the same time, as they are a product of the collapse of the oxide film, their shape should be nearly cubic, which is confirmed by the abnormally high viscosity of the composite melt studied in paper [27]. The thickness of the dynamically formed oxide film, according to [16], can be up to 100 nm; a similar result is presented in paper [17]. Thus, in the framework of the developed mathematical model, let us suppose that aluminum oxide particles have the cubic form with a facet of 100 nm and volume of 1,000,000 nm^3. The surface of aluminum oxide active to hydrogen shall be calculated on base of the parameter of the alpha-aluminum rhombic lattice 0.512 nm. The active volume is a complete cube with an outer facet 100 nm and thickness 0.512 nm. The volume of this figure is 15,281 nm^3, and correlation of the active and overall volume of aluminum oxide will be 1.528%. Basing on the data of Table 2, make calculations of hydrogen absorption on aluminum oxide molecules (Table 3). The molar mass of aluminum oxide is 102 g/mol, while that of hydrogen is 1 g/mol.

Table 3. Calculation of relation of hydrogen to active aluminum oxide in the composite.

Experiment	1	2	3	4	5
Aluminum oxide mass per 100 g, g	5.1 ± 0.1	4.3 ± 0.1	4.8 ± 0.1	4.6 ± 0.1	4.8 ± 0.1
Active aluminum oxide mass, g	0.077	0.065	0.072	0.069	0.072
Mol quantity of active aluminum oxide	0.00075	0.00063	0.00071	0.00066	0.00071
Hydrogen mass per 100 g, g	0.00263	0.00226	0.00240	0.00226	0.00241
Mol quantity of hydrogen	0.00263	0.00226	0.00240	0.00226	0.00241
Relation of hydrogen to active aluminum oxide	3.48	3.54	3.38	3.42	3.39

Thus, hydrogen absorption by the aluminum oxide surface corresponds, on average, to the correlation $Al_2O_3 \times 3.46$ H, which allows—even considering the model approximation (of the incomplete collapse of oxide spots to cubic particles)—no more than a monoatomic hydrogen layer on the aluminum oxide surface; that is, there is, in fact, the chemical absorption shown in paper [28]. The results of paper [29] also demonstrate the reduction in pore formation in the presence of small-size products of the oxide film collapse.

A polished section of the specimen with incomplete blowing possesses clear-cut hydrogen porosity. The pore size achieves 600 μm. Calculation according to formula (1) will also show a proximal yet insufficient oxide content for hydrogen absorption from the melt (11.24 as calculated versus 12.6 actual), the more so because a significant portion of the oxide spots remain undestroyed at incomplete blowing, and so the proposed model becomes inadequate. The hydrogen porosity effect in aluminum alloys contaminated by a significant quantity of finely dispersed oxides is described in [30], but the oxide surface in cast alloys is extremely small in relation to composite materials. Aluminum oxide in the melt, as with any other suspension, hinders the process of gas emission from the casting.

A polished section of the specimen without blowing demonstrates a smaller hydrogen porosity than in the case with incomplete blowing. This is due to the fact that, when a melt is loaded into a mold, the burning of hydrogen begins on the "metal-mold" interface, and a crust on the casting surface is not formed for quite a long time, thus, assuring the melt degassing. Still, gaseous porosity in the hydrogen-charged melt is present, pores have a high dispersion in their sizes, there are both pores that are 300 μm and small pores that

are 50 μm (Figure 6). A small size of hydrogen pores demonstrates the low temperature gradient during the crystallization of the casting.

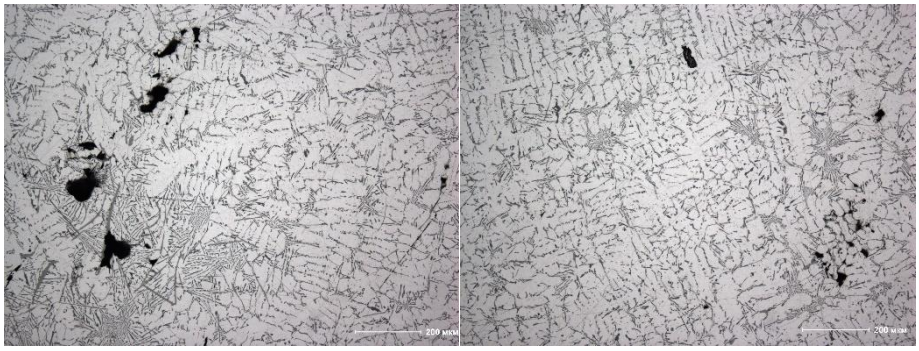

Figure 6. The alloy without blowing.

Authors should discuss the results and how they can be interpreted from the perspective of previous studies and of the working hypotheses. The findings and their implications should be discussed in the broadest context possible. Future research directions may also be highlighted.

4. Conclusions

The technology of producing a composite material by the method of the oxygen blowing of a pre-hydrogenated alloy AlSi7Fe1 allows for the production of leakless castings, which is assured by hydrogen burning out during the process of blowing on the melt mirror and the residual hydrogen absorption on oxide particles surface. When the burn out hydrogen from the melt is not complete, hydrogen porosity will be formed in the castings. The proposed method of prevention of gas porosity in cast composites is alternative to the conventional one and offers not only purging of the melt from oxide inclusions but, on the contrary, significant increase in their specific surface, which allows the reduction in hydrogen content on the inclusion surface to the monoatomic level.

Author Contributions: A.F. provided methodology and writing the manuscript, A.S. provided experimental, N.D. provided data analysis. All authors have read and agreed to the published version of the manuscript.

Funding: This research received no external funding.

Institutional Review Board Statement: Not applicable.

Informed Consent Statement: Not applicable.

Conflicts of Interest: The authors declare no conflict of interest.

References

1. Schmidt, A.; Siebeck, S.; Götze, U.; Wagner, G.; Nestler, D. Particle-Reinforced Aluminum Matrix Composites (AMCs)—Selected Results of an Integrated Technology, User, and Market Analysis and Forecast. *Metals* **2018**, *8*, 143. [CrossRef]
2. Priyadarshi, D.; Sharma, R.K. Porosity in Aluminium Matrix Composites: Cause, Effect and Defence. *Mater. Sci. Ind. J.* **2016**, *14*, 119–129.
3. Ray, S. Synthesis of Cast Metal Matrix Particulate Composites. *J. Mater. Sci.* **1993**, *28*, 5397–5413. [CrossRef]
4. Dandekar, C.R.; Shin, Y.C. Effect of Porosity on the Interface Behavior of an Al_2O_3–Aluminum Composite: A Molecular Dynamics Study. *Compos. Sci. Technol.* **2011**, *71*, 350–356. [CrossRef]
5. Borodianskiy, K.; Kossenko, A.; Zinigrad, M. Improvement of the Mechanical Properties of Al-Si Alloys by TiC Nanoparticles. *Metall. Mater. Trans. A* **2013**, *44*, 4948–4953. [CrossRef]
6. Hatch, J.E. Properties of Pure Aluminum. In *Aluminum Properties and Physical Metallurgy*; Hatch, J.E., Ed.; ASM International: Materials Park, OH, USA, 1984; pp. 1–24.
7. Tiryakioğlu, M. The Effect of Hydrogen on Pore Formation in Aluminum Alloy Castings: Myth versus Reality. *Metals* **2020**, *10*, 368. [CrossRef]

8. Kok, M. Production and Mechanical Properties of Al_2O_3 Particle-Reinforced 2024 Aluminium Alloy Composites. *JMPT* **2005**, *161*, 381–387. [CrossRef]
9. Bunk, W.; Burkhard, H.; Zabinsky, V. Beitzag zur Kenntnis des Zusammenhanges zwischen Gasgehalt und Verunreinigunen in Aluminiumschmelzen. *Z. Met.* **1968**, *59*, 757–761.
10. Schaefer, A.; Sergeev, S.; Finkelstein, A.; Chikova, O. Method of Producing Cast Composite Material No 2712675. Available online: https://www.fips.ru/publication-web/publications/document?lang=en&type=doc&tab=IZPM&id=768B749A-ED78-4038-94FA-C659A133870F (accessed on 15 January 2021).
11. Zhang, Y.; Li, R.; Zhou, X.; Cai, M.; Sun, X. Selective Growth of [alpha]-Al_2O_3 Nanowires and Nanobelts. *J. Nanomater.* **2008**, *2008*, 8. [CrossRef]
12. Newkirk, M.S.; Dizio, S.F. Novel Ceramic Materials and Methods for Making Same No. 4713360. Available online: https://patents.google.com/patent/US4713360A/en (accessed on 15 January 2021).
13. Babcsán, N.; Leitlmeier, D.; Degischer, H.P.; Banhart, J. The Role of Oxidation in Blowing Particle-Stabilised Aluminium Foams. *Adv. Eng. Mater.* **2004**, *6*, 421–428. [CrossRef]
14. Finkelstein, A.; Schaefer, A.; Chikova, O.; Borodianskiy, K. Study of Al-Si Alloy Oxygen Saturation on Its Microstructure and Mechanical Properties. *Materials* **2017**, *10*, 786. [CrossRef]
15. Nayebi, B.; Divandari, M. Characteristics of Dynamically formed Oxide Films on Molten Aluminium. *Int. J. Cast Met. Res.* **2012**, *25*, 270–276. [CrossRef]
16. Finkelstein, A.B.; Schaefer, A.; Chikova, O.A. Microstructures, mechanical properties ingot AlSi7Fe1 after blowing oxygen through melt. *Acta Metall. Slovaca* **2017**, *23*, 4–11. [CrossRef]
17. Chikova, O.A.; Finkel'shtein, A.B.; Shefer, A.A. Structure and Nanomechanical Properties of the Al–Si–Fe Alloy Produced by Blowing the Melt with Oxygen. *Phys. Met. Metallogr.* **2018**, *119*, 685–690. [CrossRef]
18. Chernyshov, E.A.; Romanov, A.D.; Romanova, E.A.; Mylnikov, V.V. Development of Technology to Produce Cast Aluminium Matrix Composite by Alumina Strengthening Phase Synthesis in Aluminium Melt. Izvestiya vuzov. *Powder Metall. Funct. Coat.* **2017**, *4*, 29–36. [CrossRef]
19. Aluminium Casting Alloys. Specifications No 1583. Available online: http://docs.cntd.ru/document/gost-1583-93 (accessed on 15 January 2021).
20. Babcsán, N.; Leitlmeier, D.; Banhart, J. Metal Foams—High Temperature Colloids: Part I. Ex Situ Analysis of Metal Foams. *Colloids Surf. A Physicochem. Eng. Asp.* **2005**, *261*, 123–130. [CrossRef]
21. Anyalebechi, P.N. Analysis of the Effects of Alloying Elements on Hydrogen Solubility in Liquid Aluminum Alloys. *Scr. Metall. Mater.* **1995**, *33*, 1209–1216. [CrossRef]
22. Aluminium Casting and Wrought Alloys. Methods for Determination of Aluminium Oxide No 11739.1. Available online: http://docs.cntd.ru/document/1200010176 (accessed on 15 January 2021).
23. Brondyke, K.J.; Hess, P.D. Interpretation of Vacuum Gas Test Results for Aluminum Alloys. *Trans. TMS-AIME* **1964**, *230*, 1542–1546.
24. Campbell, J. Porosity. In *Complete Casting Handbook: Metal Casting Processes, Metallurgy, Techniques and Design*, 2nd ed.; Gifford, C., Ed.; Butterworth-Heinemann: Oxford, UK, 2015; pp. 341–415.
25. Lu, L.; Nogita, K.; McDonald, S.D.; Dahle, A.K. Eutectic Solidification and Its Role in Casting Porosity Formation. *JOM* **2004**, *56*, 52–58. [CrossRef]
26. Dispinar, D.; Campbell, J. Porosity, Hydrogen and Bifilm Content in Al Alloy Castings. *Mater. Sci. Eng. A* **2011**, *528*, 3860–3865. [CrossRef]
27. Finkelshtein, A.B.; Chikova, O.A.; Makhmudzoda, M.; V'yukhin, V.V. Viscosity of a Liquid Al–7% Si+ 5% Al_2O_3 Aluminum Matrix Composite Material. *Russ. Metall. (Met.)* **2019**, *2019*, 809–811. [CrossRef]
28. Arbuzova, L.A.; Slovetskaya, K.I.; Rubinshtein, A.M.; Kunin, L.L.; Danilkin, V.A. Chemisorption of Hydrogen on Aluminum Oxide. *Russ. Chem. Bull.* **1971**, *20*, 148–149. [CrossRef]
29. Gyarmati, G.; Fegyverneki, G.; Mende, T.; Tokár, M. Characterization of the Double Oxide Film Content of Liquid Aluminum Alloys by Computed Tomography. *Mater. Charact.* **2019**, *157*, 1–27. [CrossRef]
30. Chen, X.G.; Gruzleski, J.E. Influence of Melt Cleanliness on Pore Formation in Aluminium—Silicon Alloys. *Int. J. Cast Met. Res.* **1996**, *9*, 17–26. [CrossRef]